

Energy Efficient Signal Acquisition in Wireless Sensor Networks : A Compressive Sensing Framework

Wei Chen and Ian J. Wassell

Digital Technology Group (DTG), Computer Laboratory, University of Cambridge, UK

Email: {wc253,ijw24}@cam.ac.uk



Abstract

The sampling rate of the sensors in wireless sensor networks (WSNs) determines the rate of its energy consumption since most of the energy is used in sampling and transmission. To save the energy in WSNs and thus prolong the network lifetime, we present a novel approach based on the compressive sensing (CS) framework to monitor 1-D environmental information in WSNs. The proposed technique is based on CS theory to minimize the number of samples taken by sensor nodes. An innovative feature of our approach is a new random sampling scheme that considers the causality of sampling, hardware limitations and the trade-off between the randomization scheme and computational complexity. In addition, a sampling rate indicator (SRI) feedback scheme is proposed to enable the sensor to adjust its sampling rate to maintain an acceptable reconstruction performance while minimizing the number of samples. A significant reduction in the number of samples required to achieve acceptable reconstruction error is demonstrated using real data gathered by a WSN located in the Hessle Anchorage of the Humber Bridge.

1 INTRODUCTION

Wireless sensor networks (WSNs) provide a flexible way to detect spatial information through a large number of sensor nodes. There are three main challenges in WSNs, i.e., lifetime, computational ability and bandwidth constraints. The first two challenges are due to size and cost limitations, as most applications require the use of small and inexpensive sensor nodes, while the third challenge results from the physical characteristic of the wireless channel. Although the sensor nodes have limited computational capability and energy, the fusion center (FC) (or any back-end processor) usually has a comparatively high computational capability [1]. The asymmetrical structure of WSNs motivates us to exploit compressive sensing (CS) related techniques and to incorporate those techniques into a WSN system for data acquisition.

CS, also called compressed sensing or Sub-Nyquist sampling [2]–[5], has a surprising property that one can recover sparse signals from far fewer samples than is predicted by the Nyquist-Shannon sampling theorem. It has been applied to medical imaging [6], [7] and compressive radar [8]–[10]. CS directly acquires the compressed signal while sampling, and so no explicit compression process is required. Samples made via CS contain a little redundancy in the information level, and the sampling process accomplishes two functions, i.e., detection and compression. CS trades-off an increase in the computational complexity of post-processing against the convenience of a smaller quantity of data acquisition and lower demands on the computational capability of the sensor node. A brief description of the reconstruction process is presented in Section 2.

The traditional approach to measure 1-D environmental information, e.g., temperature, is to uniformly sample and then report data to a FC. The sampling period could range from milliseconds to minutes depending upon the particular application. Actually, such signals are generally compressible by transforming to some suitable basis, e.g., a Fourier basis or wavelet basis. The traditional sampling approach is not energy efficient since the transmitted raw data contains a large amount of redundant information. An alternative method [11] is compressing and then transmitting. Although power consumption of the transmission is reduced in this way, the energy consumed in sampling is not changed and the compression process requires additional energy and makes computational demands of the sensor nodes. Furthermore, this approach is not suitable for real-time applications owing to the latency in gathering the data and the computation required to execute the compression algorithm at the sensor node.

In this paper, a novel approach is developed to reduce the energy consumption of sensor nodes in monitoring 1-D environmental information. The proposed technique is based on CS framework motivated by the asymmetrical structure of WSNs. Compared with the other two approaches mentioned previously, CS overcomes all the disadvantages with no penalty at the sensor, although the FC has to make a significant effort for signal recovery. The main contributions of this paper are summarized as follows. Firstly, we propose a practical random sampling generator considering the causality of sampling and hardware limitations, where the parameters of the generator can be adjusted to trade-off the randomness of sampling against fast reconstruction. We derive the closed-form expression of the expected value of the sampling interval in terms of the parameters of this random generator. Secondly, the proposed approach does not need any prior knowledge about the monitored signal to determine a suitable sampling rate, and sensors are able to adjust their sampling rates to make the reconstruction reliable for signals with time-varying sparsity levels. The details of the proposed approach are described in Section 3. Note that part of the work we present in this paper has appeared in a different form in our earlier conference publication [12].

Our objective is to provide an energy efficient methodology to enable practical low-cost, reliable WSN-based systems for monitoring 1-D environmental information. In Section 4, we use real data gathered by a WSN located in the Hessle Anchorage of the Humber Bridge [13] to evaluate the proposed approach.

Simulations show that under a specified level of reconstruction error, the number of samples and hence the energy required owing to both data acquisition and transmission can be significantly reduced by using the proposed approach.

2 COMPRESSIVE SENSING OVERVIEW

According to the Shannon sampling theorem, the sampling rate should be no less than twice the maximum frequency present in the signal. Actually, this minimum sampling rate is a worst case bound. Most natural signals can be transformed to another space, where a small number of the coefficients represent most of the power of the signals, e.g., audio signals can be transformed into the frequency domain, images can be represented by a discrete cosine transform (DCT) or transformed into the wavelet domain.

CS is an alternative sampling theory, which asserts that certain signals can be recovered from far fewer samples than Shannon sampling uses. The idea of CS is that a signal $\mathbf{f} \in \mathbb{R}^N$ can be recovered from a small set of M ($M \ll N$) non-adaptive, linear measurements $\mathbf{y} \in \mathbb{R}^M$ if the signal can be represented as a sparse objective $\mathbf{x} \in \mathbb{R}^N$ in some orthonormal basis $\Psi \in \mathbb{R}^{N \times N}$. The sampled signal via CS can be presented as

$$\mathbf{y} = \Phi \mathbf{f} + \mathbf{z} = \Phi \Psi \mathbf{x} + \mathbf{z}, \quad (1)$$

where $\Phi \in \mathbb{R}^{M \times N}$ represents a sensing matrix and \mathbf{z} is an unknown noise term.

The success of CS relies on two objective conditions, i.e., sparsity and incoherence. Sparsity makes it possible to abstract the signal with less samples than the Shannon sampling theory requires. We say the signal \mathbf{f} is S sparse if $\mathbf{x} \in \mathbb{R}^N$ has only S nonzero elements. CS can also be used to approximately reconstruct a nearly sparse signal with power-law distributions, i.e., the i th largest entry of the transformed representation satisfies

$$|x_i| \leq C_0 \cdot i^{-p} \quad (2)$$

for each $1 \leq i \leq N$, where C_0 is a constant and $p \geq 1$. In addition, incoherence between the sensing matrix Φ and the transform system Ψ is also of crucial importance for CS. Random matrices are largely incoherent with any fixed basis [4], which makes CS a general strategy for sampling.

To check whether a specific sensing matrix is qualified for recovering a sparse signal, the usual criterion employed is the restricted isometry property (RIP). Formally, a matrix \mathbf{A} of size $M \times N$ is said to satisfy the RIP of order S with a restricted isometry constant (RIC) $\delta_S \in (0, 1)$ being the smallest number such that

$$(1 - \delta_S) \|\mathbf{x}\|_2^2 \leq \|\mathbf{A}\mathbf{x}\|_2^2 \leq (1 + \delta_S) \|\mathbf{x}\|_2^2 \quad (3)$$

holds for all \mathbf{x} with $\|\mathbf{x}\|_0 \leq S$, where $\|\mathbf{x}\|_0$ denotes the number of non-zero elements in \mathbf{x} , and we define the ℓ_p norm of the vector \mathbf{x} as $\|\mathbf{x}\|_p^p = \sum_{i=1}^N |x_i|^p$. It has been established that the RIP provides a sufficient condition for exact or near exact recovery of a sparse signal via ℓ_1 minimization. Various conditions on the RIC are derived in [14]–[17].

For a given sensing matrix, it is NP-hard to find out if it satisfies the RIP with a specific RIC δ_S [3]. However, it has been established that a random $M \times N$ matrix, whose entries are i.i.d. realizations of certain zero-mean random variables with variance $\frac{1}{M}$, satisfies the RIP with a high probability when $M \geq \text{const} \cdot S \log \frac{N}{S}$ [18]. Thus, $\mathcal{O}(S \log \frac{N}{S})$ random linear measurements are enough to reliably recover a signal where the number of nonzero coefficients is no more than S .

Since it is a linear program (LP) [3], ℓ_1 minimization is widely used for CS signal reconstruction, while ℓ_0 minimization is computationally intractable. One form of reconstruction using the ℓ_1 minimization is known as basis pursuit de-noise (BPDN) [19], which can be written as

$$\begin{aligned} \min_{\hat{\mathbf{x}}} \quad & \|\hat{\mathbf{x}}\|_1 \\ \text{s.t.} \quad & \|\Phi\Psi\hat{\mathbf{x}} - \mathbf{y}\|_2 \leq \epsilon, \end{aligned} \quad (4)$$

where ϵ is an estimate of the noise level. In [14], Candès shows that CS is robust to the effect of noise since the solution \mathbf{x}^* of (4) obeys

$$\|\mathbf{x}^* - \mathbf{x}\|_2 \leq C_1 S^{-1/2} \|\mathbf{x} - \mathbf{x}_S\|_1 + C_2 \epsilon, \quad (5)$$

where $C_1 = \frac{2+(2\sqrt{2}-2)\delta_{2S}}{1-(\sqrt{2}+1)\delta_{2S}}$, $C_2 = \frac{4\sqrt{1+\delta_{2S}}}{1-(\sqrt{2}+1)\delta_{2S}}$, \mathbf{x}_S is an approximation of \mathbf{x} with all but the S -largest entries set to zero, and δ_{2S} is the RIC of matrix $\Phi\Psi$.

Another form of reconstruction in the presence of noise is known as the least absolute shrinkage and selection operator (LASSO) [20], which instead minimizes the energy of detection error with an ℓ_1 constraint:

$$\begin{aligned} \min_{\hat{\mathbf{x}}} \quad & \|\Phi\Psi\hat{\mathbf{x}} - \mathbf{y}\|_2^2 \\ \text{s.t.} \quad & \|\hat{\mathbf{x}}\|_1 \leq \eta, \end{aligned} \quad (6)$$

where $\eta \geq 0$. Both BPDN and LASSO can be written as an unconstrained optimization problem for some $\tau \geq 0$ for any $\eta \geq 0$ and $\epsilon \geq 0$:

$$\min_{\hat{\mathbf{x}}} \quad \frac{1}{2} \|\Phi\Psi\hat{\mathbf{x}} - \mathbf{y}\|_2^2 + \tau \|\hat{\mathbf{x}}\|_1. \quad (7)$$

Many algorithms and their variants have been proposed in the literature. Most of these algorithms can be classified into two categories: convex optimization algorithms and greedy algorithms. There are several methods in the category of convex optimization to search for the global optimal solution such as the steepest descent and the conjugate gradient (CG). Interior point (IP) methods, developed in the 1980s to solve convex optimization, are used in [19], [21], [22] for sparse reconstruction. Figueiredo, Nowak and Wright proposed a gradient projection (GPSR) approach with one level of iteration [23], while the IP approaches in [19], [21] have two iteration levels and ℓ_1 -magic [22] has three iteration levels. The second class of convex optimization approaches to solve the unconstrained optimization problem (7) use the homotopy method [24]–[26]. The homotopy method has a property that the number of iterations is equal to the number of nonzero coefficients of the signal. Thus, it is much faster in applications having a small

number of nonzero components. However, the homotopy method is impractical in high-dimensional problems that contain a large number of nonzero coefficients. The second category of CS recovery algorithms are greedy methods that are not based on optimization. This category includes a number of algorithms such as matching pursuit (MP) [27], Orthogonal Matching Pursuits (OMP) [28], Stagewise Orthogonal Matching Pursuit (StOMP) [29], regularized orthogonal matching pursuit (ROMP) [30], compressive sampling matching pursuit (CoSaMP) [31] and Subspace Matching Pursuit [32]. The idea of these algorithms is to iteratively compute part of the support, i.e., the non-zero elements of the sparse signal, and to recover the sparse signal using the sensing matrix with columns corresponding to the support. The major advantages of this method are speed and ease of implementation.

However, it is almost impossible to determine the minimum number of measurements beforehand to guarantee a successful reconstruction with a particular algorithm. For one thing, one cannot acquire the exact number of nonzero elements, or the sparsity level of the sparse representation without the signal in hand. Although one could use empirical knowledge of the sparsity level in some particular applications in order to decide upon the number of measurements required, the reconstruction will fail when the sparsity level is time-varying, not to mention the situation where the empirical knowledge is incorrect. Also, even if one knows the sparsity level, it is still impossible to identify the minimum number M of random measurements needed. In fig 1, we illustrate the distribution of the minimum number M of measurements for random Gaussian sensing matrices in a zero-noise scenario, where the sparse signal ($N = 200$) contains $S = 10$ randomly placed ± 1 spikes. We use the ℓ_1 -magic reconstruction algorithm [22] for (4) with over 1000 experimental trials. As is readily apparent in the figure, the minimum number of measurements has a high variance for a given sparse signal. Therefore, for practical applications, it is crucial to have the capability to estimate the reconstruction performance and adaptively adjust the sampling rates in order to maintain an acceptable reconstruction performance.

3 THE PROPOSED COMPRESSIVE SENSING APPROACH

In this section, we present a novel CS approach for a WSN to monitor 1-D environmental information. In our CS setting, we assume no knowledge about the sparsity level of the signal and the sparsity level could be time-varying. The proposed approach includes three main process, i.e., random sampling at the sensor, CS reconstruction at the FC and sampling rate indicator (SRI) feedback from the FC to sensors.

3.1 Causal Random Sampling

The technique to be used here is known as random sampling, which was successfully applied in [33], [34]. Sampling at uniformly distributed random time points satisfies the RIP when the sparse basis Ψ is orthogonal [35]. For random sampling of 1-D signals, the entries of the sensing matrix Φ are all zeros except for M entries in M different columns and rows. To maintain the causality of the sampling process,

the order of the M unity entries in different rows should be sorted by the column number, e.g.,

$$\Phi = \begin{bmatrix} 0 & 1 & 0 & 0 & 0 & 0 & \cdots & 0 \\ 0 & 0 & 1 & 0 & 0 & 0 & \cdots & 0 \\ 0 & 0 & 0 & 0 & 0 & 1 & \cdots & 0 \\ & & & \vdots & & & \ddots & \vdots \\ 0 & 0 & 0 & 0 & 0 & 0 & \cdots & 1 \end{bmatrix}.$$

However, randomized sampling cannot be applied directly to a real WSN since two sampling times may be too close to be handled by the hardware. To overcome this, Dang, et al. generate random indexes in a short time period and scale them to a larger time scale [34]. To increase the sampling time randomness, they embed a normally distributed time jitter to the result. The sampling time $\mathbf{t} \in \mathbb{R}^{M \times 1}$ in [34] can be expressed by the following equation:

$$\begin{aligned} \mathbf{t} = & \alpha \times \text{randsample}\left(\frac{N}{\omega}, M\right) \\ & + \beta \times \text{round}(\text{randn}(M, 1)), \end{aligned} \quad (8)$$

where α is the down sampling factor, N is the maximum number of samples limited by the hardware, M the number of samples we actually take, β is scaling factor of the jitter, ω is a positive number, function $\text{randsample}(\frac{N}{\omega}, M)$ randomly picks M numbers from 1 to $\frac{N}{\omega}$, function $\text{randn}(M, 1)$ generates an $M \times 1$ matrix with i.i.d. normally distributed entries satisfying $N(0, 1)$, function $\text{round}(c)$ rounds c to the nearest integer, i.e., $\lfloor x + 0.5 \rfloor$ for positive c and $\lfloor x - 0.5 \rfloor$ for negative c and $\lfloor \cdot \rfloor$ denotes the flooring function. Another simpler approach to solve this issue is to use the additive random sampling process [36]. In this case, the sampling time is

$$t_i = t_{i-1} + \alpha_i, \quad (9)$$

where $i \in [1, M]$, $t_0 = 0$, α_i is an i.i.d. Gaussian random variable $\sim N(\frac{N}{M}, \frac{r^2 N^2}{M^2})$ where the constant r determines the speed of convergence. The authors of [36] use $r = 0.25$ in their implementation and force α_i to be larger than the analogue to digital conversion (ADC) sampling latency.

These two methods allow sampling at arbitrary times that is suitable for the hardware. Thus, the minimum interval could be one time unit, which leads to a high resolution and puts the burden onto the FC. For some application, e.g., environmental temperature monitoring, one often does not need a very high resolution. To trade-off the randomness of sampling against faster computation, the sampling intervals could be several multiples of a given time unit. Let ε denote the minimum sampling interval that the hardware can use and μ be a fixed positive integer. A large value of μ trades-off randomization for the convenience of the FC. We suggest a simpler approach for sampling that can be written as follows

$$t_i = t_{i-1} + \lceil \gamma_i \rho \rceil \mu \varepsilon, \quad (10)$$

where $\rho > 1$, γ_i is an i.i.d. random variable with the distribution $\mathcal{U}(0, 1)$ and function $\lceil c \rceil$ gives the smallest integer no less than c . The average sampling rate is equal to the multiplicative inverse of the

expected value of the sampling interval $t_{i+1} - t_i$, which can be written as

$$\begin{aligned}
 AVE &= \int_0^1 \lceil \gamma \rho \rceil \mu \varepsilon \cdot d\gamma \\
 &= \frac{\mu \varepsilon}{\rho} \int_0^\rho \lceil \gamma \rceil \cdot d\gamma \\
 &= \frac{\lceil \rho \rceil (2\rho - \lceil \rho \rceil + 1)}{2\rho} \mu \varepsilon.
 \end{aligned} \tag{11}$$

We note that AVE is a monotonically increasing function of ρ . With any given value of ρ , one can calculate the average sampling rate using (11). Inversely, for a given sampling rate, one can find the value of ρ by using a look-up table. To compare with traditional sampling, one would like the average sampling interval to be equal to $\frac{N}{M} \mu \varepsilon$, which results in $\rho \approx \frac{2N}{M} - 1$. In fig 2, we illustrate the difference between $\frac{N}{M} \mu \varepsilon$ and AVE with $\rho = \frac{2N}{M} - 1$ by calculating $\text{diff} = \frac{AVE - \frac{N}{M} \mu \varepsilon}{\mu \varepsilon}$. As is apparent in the graph, the average sampling interval is quite close to the target value $\frac{N}{M} \mu \varepsilon$, which means one could use $\rho = \frac{2N}{M} - 1$ in (10) where the average sampling interval is close to $\frac{N}{M} \mu \varepsilon$. The sensor is notified of the value of ρ by the FC using a procedure that we will describe later in Section 3.3.

3.2 CS On-line Reconstruction

CS algorithms can recover an off-line signal that has a sparse representation having relatively few samples. Employing the same approach to deal with an on-line signal such as the instantaneous temperature of the environment, the FC starts each reconstruction when enough new samples are gathered. Thus, the latency of this approach is the time taken to gather the data. However, many applications of interest for sensor networks require timely feedback based on the latest information concerning the environment. The off-line approach that has a long response delay is not suitable for these applications.

Ideally, for an on-line application, the FC should make the reconstruction and report the update when it receives each new sample. The response delay of this ideal method is given by the random sampling interval. To reconstruct a signal within a very short sampling interval, the FC must have the power of a super computer even using up to date reconstruction algorithms. To trade-off the response delay for lower computational requirements, one possibility is to perform a reconstruction after receiving several new samples. Both the new samples and a number of prior samples are then used to recover the signal. The period of reconstruction should be chosen to be less than the required delay sensitivity of the specific application, and longer than the time that one reconstruction process consumes.

3.3 SRI Feedback

We define $SRI = \rho$, where the expected sampling rate is equal to $\frac{2\rho}{\lceil \rho \rceil (2\rho - \lceil \rho \rceil + 1) \mu \varepsilon}$ according to (11). As we discussed previously, one could use $\rho = \frac{2N}{M} - 1$ to make the average sampling interval approximate to $\frac{N}{M}$ or look it up in a table for a precise value. The sensor does not require prior information about the

sparsity level of the signal to determine the value of SRI. The SRI feedback enables the sensor to adjust its sampling rate to keep the reconstruction quality within an acceptable range.

This SRI feedback scheme is illustrated in fig 3. At the beginning, the sensor sends its pseudo-random generator seed to the FC. Then it samples the unknown signal at its highest rate and sends the samples to the FC until the SRI feedback is received. The FC calculates the sparsity level of the received samples. If a sparse representation is found, the FC use a decreased number of samples for reconstruction until the reconstruction quality indicator (RQI) falls into a desired specified range. Then the FC will send the SRI back to the sensor to let it adjust its sampling rate. When the RQI goes out of the range, the sensor will be notified to increase or decrease its random sampling rate via the SRI until the RQI again becomes acceptable. This scheme enables the sensor to sample any 1-D environmental signal blindly and then adaptively adjust its sampling rate when unanticipated changes of the sparsity level of the monitored signal occur.

However, how can we compute the reconstruction quality directly without explicitly knowing the whole signal? What we propose is to use L additional reserved samples to evaluate the reconstruction performance. The use of these additional samples can be viewed in a similar way to that of pilot symbols in a communication system. The recovered signal is compared with the reserved samples to determine the SRI. The FC compares the reserved data with the corresponding reconstructed data for calculating the RQI, which is defined as

$$RQI = \frac{\|\hat{\mathbf{f}}_{\mathcal{J}} - \mathbf{y}_{\mathcal{J}}\|_2^2}{\|\mathbf{y}_{\mathcal{J}}\|_2^2}, \quad (12)$$

where \mathcal{J} is the index set of the reserved samples, $\hat{\mathbf{f}}_{\mathcal{J}} \in \mathbb{R}^L$ is the truncated reconstructed signal corresponding to the reserved samples, and $\mathbf{y}_{\mathcal{J}} \in \mathbb{R}^L$ is the vector of reserved samples. If the RQI is below the acceptable reconstruction quality, the FC will send an SRI message to make sensor increase its sampling rate. Conversely, if the RQI is above the upper threshold, the sensor will be notified to decrease the sampling rate to reduce energy consumption.

The number of reserved measurements depends upon the desired accuracy of estimation ζ and the confidence level ν in the prediction and the bound is given as follows:

Theorem 1 [37]: Fix an accuracy parameter $\zeta \in (0, \frac{1}{2}]$, a confidence parameter $\nu \in (0, 1)$ and a vector $\mathbf{x} \in \mathcal{R}^N$. Let \mathbf{B} be an $J \times N$ matrix of Gaussian or Bernoulli type. If $J \geq C\zeta^{-2} \log(1/2\nu)$, then the estimate $\hat{\mathbf{x}} \in \mathcal{R}^N$ satisfies

$$\frac{1 - 3\zeta}{(1 + \zeta)(1 - \zeta)^2} \frac{\|\mathbf{B}(\mathbf{x} - \hat{\mathbf{x}})\|_2}{\|\mathbf{B}\mathbf{x}\|_2} \leq \frac{\|\mathbf{x} - \hat{\mathbf{x}}\|_2}{\|\mathbf{x}\|_2} \leq \frac{1}{(1 - \zeta)^2} \frac{\|\mathbf{B}(\mathbf{x} - \hat{\mathbf{x}})\|_2}{\|\mathbf{B}\mathbf{x}\|_2} \quad (13)$$

with probability exceeding $1 - \nu$.

Remark: This bound is derived in terms of a sensing matrix of either Gaussian or Bernoulli type using the Johnson-Lindenstrauss (JL) lemma [38]. For a specified confidence ν , the accuracy could be written as a function $\zeta(J)$ of the number of measurements for validation, where $C = 1$ upper bounds the optimal

constant for the sensing matrix of those two types [37]. In [39], the estimation accuracy is evaluated in the case of a sensing matrix with i.i.d. Gaussian entries.

For random sampling of 1-D signals, one may consider the sensing matrix as a short-time Fourier transform, a curvelet transform, a wavelet transform and so on. In this paper, we take a truncated Fourier matrix as an example. We define the RQI scaling factor as

$$RQI \text{ scaling factor} = \frac{\left\| \hat{\mathbf{f}}_{\mathcal{J}} - \mathbf{y}_{\mathcal{J}} \right\|_2^2 / \|\mathbf{y}_{\mathcal{J}}\|_2^2}{\left\| \hat{\mathbf{f}} - \mathbf{f} \right\|_2^2 / \|\mathbf{f}\|_2^2}, \quad (14)$$

which represents the accuracy of using reserved measurements to predict the reconstruction performance. Fig 4 plots the RQI scaling factor against the number of reserved samples. In this experiment, we generate the nearly sparse signal \mathbf{x} and its estimation $\hat{\mathbf{x}}$ with $N = 1024$ and power-law distributions. We note the RQI is approaching the actual reconstruction quality with an increased number of partial Fourier measurements. Fig 5 shows the distributions of the RQI scaling factor of signals with different lengths ($N = 256, 512$ and 2048), where 10% of the samples of the signal are reserved for validation, while the other settings are the same as the previous experiment. We plot a histogram of the RQI scaling factor for each signal over 10000 trials. We note from inspection of fig 5 that this approach turns to be more efficient for large N in terms of the required ratio of reserved samples for some acceptable accuracy.

Although the reconstructed signal would be accurate enough even without using the reserved samples, one can have a more accurate result by using all of the samples for reconstruction. In this way, there is no waste of samples, even if one keeps a small portion of them for validating the earlier reconstruction.

4 PERFORMANCE EVALUATION

In this section, we provide an example to show the performance of the proposed CS approach described in the previous section. All the data we use were gathered by the wireless environmental sensor network located in the Hessle Anchorage of the Humber Bridge [13] from 08/09/2007 06:25:00 to 15/10/2007 05:39:46. Fig 6 shows the layout of the WSN, where 11 MicaZ sensing nodes with temperature sensors were deployed. The temperature of the environment are sensed and reported to the FC, while some of the samples are lost during the transmission. We demonstrate that the proposed approach can significantly reduce the number of samples needed for representing the environmental information under a required reconstruction quality.

In our evaluation, each sampling time is derived from equation (10). We use the interior point algorithm in ℓ_1 -magic [22] for solving (4) with $\epsilon = 10^{-3}$. Fig 7 shows the first segment of original temperature signal, which has 2000 samples and is then randomly sampled at different rates. In this example, 90% of the samples are used for CS reconstruction, while the remaining 10% samples are reserved for evaluation of the reconstruction quality. We compute the RQI at different sampling rates and average it over 100 independent trials, giving the results shown in fig 8. We notice that the RQI decreases as the sampling

rate is increased, i.e., the reconstruction quality is better at higher rates. However, we also notice that the RQI trend has a floor effect owing to the sampling noise in the samples reserved for comparison, which cannot be computed or estimated.

For a given RQI requirement, the FC will notify the sensor of the SRI, which can later be changed if a different reconstruction performance is needed. In this example, we require that the RQI is less than 4×10^{-7} and higher than 1×10^{-7} . According to fig 8, the system could be sampled adequately using only 10% of the original samples by CS. For the second segment of the temperature signal, the sensor reduces its random sampling rate to one fourth of its prior rate, i.e., 500 samples out of 2000 original samples, where 90% are used for reconstruction and the other 10% are reserved for calculating the RQI.

Fig 9 plots the original and the recovered temperature signals for comparison, where the RQI is 2.8×10^{-7} . Since the RQI is acceptable, no SRI feedback is given to the sensor so the sensor maintains this sampling rate. It shows that the recovered signal closely approximates the original signal. Fig 10 plots the Fourier transform coefficients of the original temperature data and the reconstructed temperature data. The coefficients are sorted in the order of magnitude for enhanced visibility. We note that the original temperature coefficients are nearly sparse and that the large coefficients are retained in the CS approach. For this example, we do not present more results for the remaining temperature data owing to their similarity to those already shown. We point out that for some scenarios, the sparsity level of the signal may vary very little in time, consequently the FC only need to send the SRI occasionally when its value moves out of the acceptable range.

5 CONCLUSION

In this paper, the proposed approach exploits the compressibility of the signal to reduce the number of samples required to recover the sampled signal at the fusion center (FC) and so reduce the energy consumption of the sensors in both sampling and transmission. We show this approach can reduce to a quarter the number of samples required to be taken in the WSN located in the Hessel Anchorage of the Humber Bridge. Consequently, the energy required for sampling and transmission can be reduced to a quarter of its original value. Although these performance results are specific to this WSN and application, the insight from these results can be applied more generally.

6 ACKNOWLEDGMENTS

The authors would like to thank Andrew Rice and Robert Harle for their valuable comments on this work, and the anonymous reviewers for their help in improving the quality of this paper.

REFERENCES

- [1] I. Akyildiz, W. Su, Y. Sankarasubramaniam, and E. Cayirci, "Wireless sensor networks: a survey," *Computer networks*, vol. 38, no. 4, pp. 393–422, 2002.

- [2] D. Donoho, "Compressed sensing," *Information Theory, IEEE Transactions on*, vol. 52, no. 4, pp. 1289–1306, 2006.
- [3] R. Baraniuk, "Compressive sensing," *Signal Processing Magazine, IEEE*, vol. 24, no. 4, pp. 118–121, 2007.
- [4] E. Candes and M. Wakin, "An introduction to compressive sampling," *Signal Processing Magazine, IEEE*, vol. 25, no. 2, pp. 21–30, 2008.
- [5] J. Haupt, W. Bajwa, M. Rabbat, and R. Nowak, "Compressed sensing for networked data," *Signal Processing Magazine, IEEE*, vol. 25, no. 2, pp. 92–101, 2008.
- [6] X. Qu, X. Cao, D. Guo, C. Hu, and Z. Chen, "Combined sparsifying transforms for compressed sensing mri," *Electronics Letters*, vol. 46, no. 2, pp. 121–123, 2010.
- [7] O. Michailovich, Y. Rathi, and S. Dolui, "Spatially regularized compressed sensing for high angular resolution diffusion imaging," *Medical Imaging, IEEE Transactions on*, vol. 30, no. 5, pp. 1100–1115, May 2011.
- [8] Y. Lin, B. Zhang, W. Hong, and Y. Wu, "Along-track interferometric sar imaging based on distributed compressed sensing," *Electronics Letters*, vol. 46, no. 12, pp. 858–860, 2010.
- [9] Y. Liu, M. Wu, and S. Wu, "Fast omp algorithm for 2d angle estimation in mimo radar," *Electronics Letters*, vol. 46, no. 6, pp. 444–445, 2010.
- [10] Y. Yu, A. Petropulu, and H. Poor, "Measurement matrix design for compressive sensing based mimo radar," *Signal Processing, IEEE Transactions on*, vol. PP, no. 99, p. 1, 2011.
- [11] T. Hamamoto, S. Nagao, and K. Aizawa, "Real-time objects tracking by using smart image sensor and fpga," in *Image Processing. 2002. Proceedings. 2002 International Conference on*, vol. 3, 2002, pp. III–441 – III–444 vol.3.
- [12] W. Chen and I. J. Wassell, "Energy efficient signal acquisition via compressive sensing in wireless sensor networks," in *Wireless Pervasive Computing, 2011. ISWPC 2011. 6th International Symposium on*, 2011.
- [13] (2009, Jun.). [Online]. Available: <http://www.bridgeforum.com/humber/hessle-anchorage-cal.php>
- [14] E. Candès, "The restricted isometry property and its implications for compressed sensing," *Comptes rendus-Mathématique*, vol. 346, no. 9–10, pp. 589–592, 2008.
- [15] S. Foucart and M. Lai, "Sparsest solutions of underdetermined linear systems via ℓ_q -minimization for $0 < q \leq 1$," *Applied and Computational Harmonic Analysis*, vol. 26, no. 3, pp. 395–407, 2009.
- [16] M. Davies and R. Gribonval, "Restricted Isometry Constants where ℓ_p sparse recovery can fail for $0 < p \leq 1$," *Information Theory, IEEE Transactions on*, vol. 55, no. 5, pp. 2203–2214, 2009.
- [17] T. Cai, L. Wang, and G. Xu, "New bounds for restricted isometry constants," *Information Theory, IEEE Transactions on*, vol. 56, no. 9, pp. 4388–4394, 2010.
- [18] R. Baraniuk, M. Davenport, R. DeVore, and M. Wakin, "A simple proof of the restricted isometry property for random matrices," *Constructive Approximation*, vol. 28, no. 3, pp. 253–263, 2008.
- [19] S. Chen, D. Donoho, and M. Saunders, "Atomic decomposition by basis pursuit," *SIAM review*, vol. 43, no. 1, pp. 129–159, 2001.
- [20] R. Tibshirani, "Regression shrinkage and selection via the lasso," *Journal of the Royal Statistical Society. Series B (Methodological)*, vol. 58, no. 1, pp. 267–288, 1996.
- [21] S. Kim, K. Koh, M. Lustig, S. Boyd, and D. Gorinevsky, "An interior-point method for large-scale ℓ_1 -regularized least squares. Selected Topics in Signal Processing," *Selected Topics in Signal Processing, IEEE Journal of*, vol. 1, no. 4, pp. 606–617, 2007.
- [22] (2009, Nov.). [Online]. Available: <http://users.ece.gatech.edu/~justin/l1magic/>
- [23] M. Figueiredo, R. Nowak, and S. Wright, "Gradient projection for sparse reconstruction: Application to compressed sensing and other inverse problems," *Selected Topics in Signal Processing, IEEE Journal of*, vol. 1, no. 4, pp. 586–597, 2007.
- [24] D. Malioutov, M. Cetin, and A. Willsky, "Homotopy continuation for sparse signal representation," in *Acoustics, Speech, and Signal Processing, 2005. Proceedings. (ICASSP '05). IEEE International Conference on*, vol. 5, 2005, pp. v/733 – v/736 Vol. 5.
- [25] D. Donoho and Y. Tsaig, "Fast Solution of ℓ_1 -Norm Minimization Problems When the Solution May Be Sparse," *Information Theory, IEEE Transactions on*, vol. 54, no. 11, pp. 4789–4812, 2008.
- [26] P. Garrigues and L. E. Ghaoui, "An homotopy algorithm for the lasso with online observations," in *Advances in Neural Information Processing Systems 21*, 2009, pp. 489–496.

- [27] S. Mallat and Z. Zhang, "Matching pursuits with time-frequency dictionaries," *IEEE Transactions on signal processing*, vol. 41, no. 12, pp. 3397–3415, 1993.
- [28] Y. Pati, R. Rezaifar, and P. Krishnaprasad, "Orthogonal matching pursuit: recursive function approximation with applications to wavelet decomposition," in *Signals, Systems and Computers, 1993. 1993 Conference Record of The Twenty-Seventh Asilomar Conference on*, Nov. 1993, pp. 40–44 vol.1.
- [29] D. Donoho, Y. Tsaig, I. Drori, and J. Starck, "Sparse solution of underdetermined linear equations by stagewise orthogonal matching pursuit," *preprint*, 2006.
- [30] D. Needell and R. Vershynin, "Uniform uncertainty principle and signal recovery via regularized orthogonal matching pursuit," *Foundations of computational mathematics*, vol. 9, no. 3, pp. 317–334, 2009.
- [31] D. Needell and J. Tropp, "CoSaMP: Iterative signal recovery from incomplete and inaccurate samples," *Applied and Computational Harmonic Analysis*, vol. 26, no. 3, pp. 301–321, 2009.
- [32] W. Dai and O. Milenkovic, "Subspace pursuit for compressive sensing: Closing the gap between performance and complexity," 2008.
- [33] F. A. Boyle, J. Haupt, G. L. Fudge, and C.-C. A. Yeh, "Detecting signal structure from randomly-sampled data," in *Statistical Signal Processing, 2007. SSP '07. IEEE/SP 14th Workshop on*, 2007, pp. 326–330.
- [34] T. Dang, N. Bulusu, and W. Hu, "Lightweight acoustic classification for cane-toad monitoring," in *Signals, Systems and Computers, 2008 42nd Asilomar Conference on*, 2008, pp. 1601–1605.
- [35] M. Rudelson and R. Vershynin, "On sparse reconstruction from Fourier and Gaussian measurements," *Communications on Pure and Applied Mathematics*, vol. 61, no. 8, pp. 1025–1045, 2008.
- [36] Z. Charbiwala, Y. Kim, S. Zahedi, J. Friedman, and M. B. Srivastava, "Energy efficient sampling for event detection in wireless sensor networks," in *Proceedings of the 14th ACM/IEEE international symposium on Low power electronics and design*, ser. ISLPED '09. New York, NY, USA: ACM, 2009, pp. 419–424.
- [37] R. Ward, "Compressed sensing with cross validation," *Information Theory, IEEE Transactions on*, vol. 55, no. 12, pp. 5773–5782, 2009.
- [38] J. Matoušek, "On variants of the Johnson–Lindenstrauss lemma," *Random Structures & Algorithms*, vol. 33, no. 2, pp. 142–156, 2008.
- [39] D. Malioutov, S. Sanghavi, and A. Willsky, "Sequential compressed sensing," *Selected Topics in Signal Processing, IEEE Journal of*, vol. 4, no. 2, pp. 435–444, 2010.

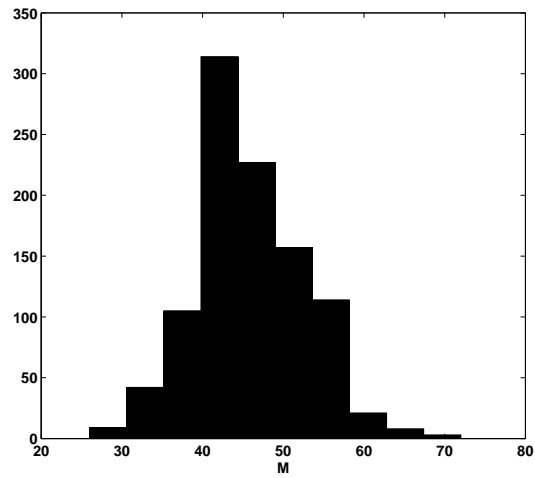


Fig. 1. Histogram of the minimum number of measurements for random Gaussian matrices ($N = 200$ and $S = 10$).

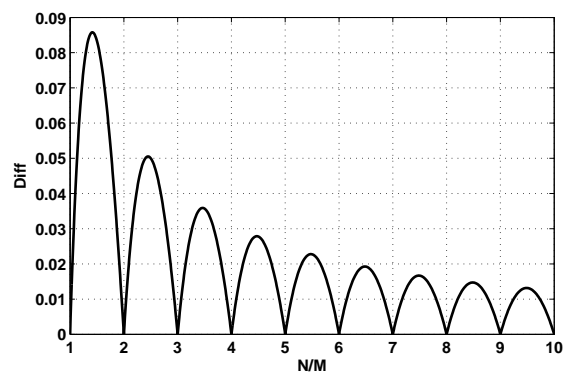


Fig. 2. The difference between $\frac{N}{M}\mu\epsilon$ and the average sampling interval with $\rho = \frac{2N}{M} - 1$.

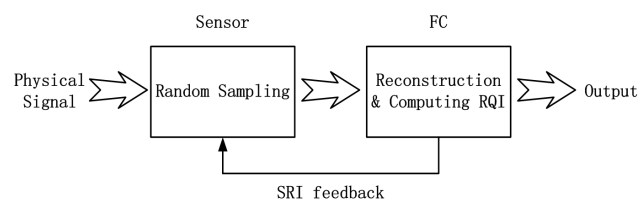


Fig. 3. The proposed CS approach.

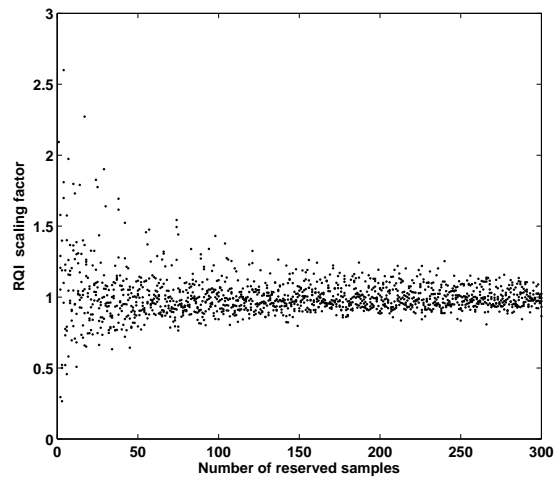


Fig. 4. RQI scaling factor ($N = 1024$).

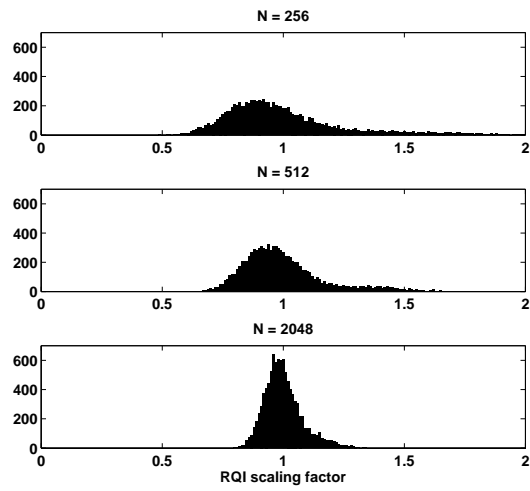


Fig. 5. Histogram of the RQI scaling factor ($\frac{J}{N} = 10\%$).

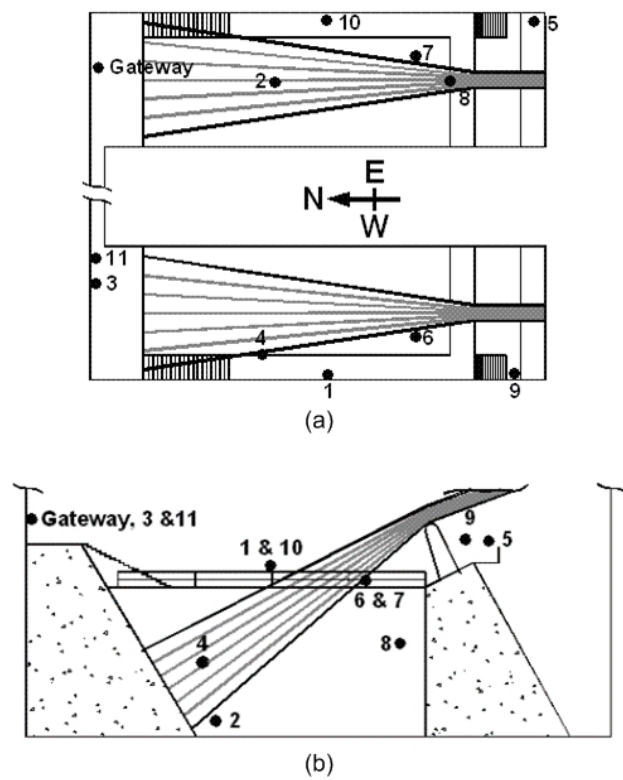


Fig. 6. Layout of the WSN at the hessle anchorage of the Humber Bridge: (a) Plan view of the WSN; (b) Elevation view of the WSN.

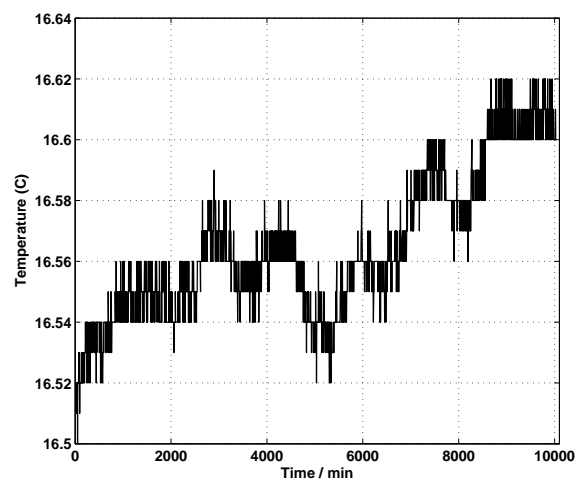


Fig. 7. The first segment of original temperature samples.

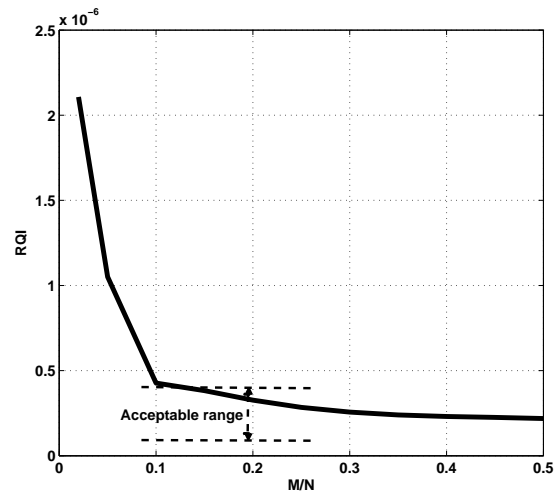


Fig. 8. The RQI trend of the first segment of the original temperature samples.

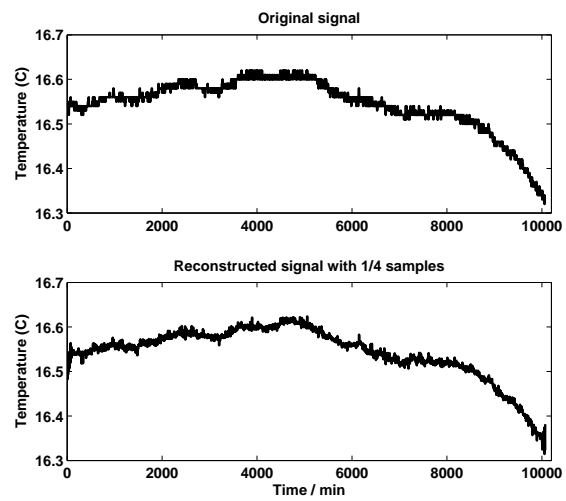


Fig. 9. The second segment of original temperature (top) and reconstructed temperature (bottom).

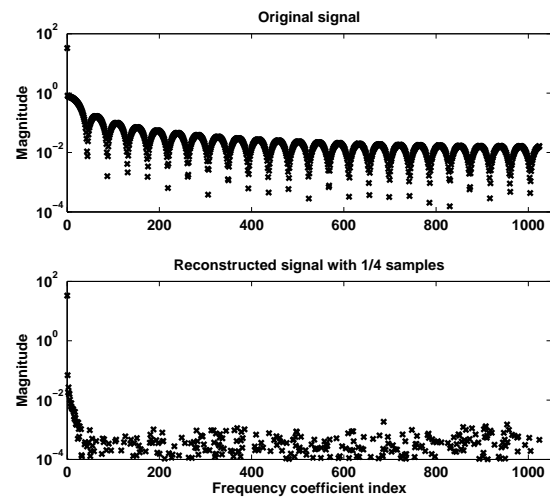


Fig. 10. Sorted Fourier transform coefficients of the second segment of original temperature (top) and reconstructed temperature (bottom).